Revised Version

MADPH-97-1025
UCD-97-22
MSUHEP-70930

UCD-97-22
MADPH-97-1025
MSUHEP-70930
hep-ph/9711429
November 1997

Quartic Gauge Boson Couplings at Linear Colliders

— Interplay of WWZ/ZZZ Production and WW-Fusion —

Tao Han [1,2] *, Hong-Jian He [3,4] †, C.–P. Yuan [4] ‡

[1] *Department of Physics, University of California*
Davis, California 95616, USA
[2] *Department of Physics, University of Wisconsin*
Madison, Wisconsin 53706, USA

[3] *Theory Division, Deutsches Elektronen-Synchrotron DESY*
D-22603 Hamburg, Germany

[4] *Department of Physics and Astronomy, Michigan State University*
East Lansing, Michigan 48824, USA

Abstract

We study new physics effects to the quartic gauge boson couplings formulated by the electroweak chiral Lagrangian. Five next-to-leading order operators characterize the anomalous quartic gauge interactions which involve pure Goldstone boson dynamics for the electroweak symmetry breaking. We estimate the typical size of these couplings in different strongly-interacting models and examine the sensitivity to directly probing them via the WWZ/ZZZ triple gauge boson production at the high energy linear colliders. The important roles of polarized e^- and e^+ beams are stressed. We then compare the results with those from the W-pair production of the WW-fusion processes, and analyze the interplay of these two production mechanisms for an improved probe of the quartic gauge boson interactions.

PACS number(s): 11.30.Qc, 11.15.Ex, 12.15.Ji, 14.70.–e

Physics Letters B (1998), in press.

*Email: THan@Ucdhep.Ucdavis.Edu
†Email: HJHe@Desy.De HJHe@Pa.Msu.Edu
‡Email: Yuan@Pa.Msu.Edu

1. Electroweak Symmetry Breaking and Quartic Gauge Boson Couplings

The validity of the Standard Model (SM) has been tested to a great precision up to the scale of $O(100)$ GeV [1], while the electroweak symmetry breaking (EWSB) mechanism remains undetermined. If the EWSB sector is weakly coupled, such as in the supersymmetric theories, the effects of new physics at higher mass scales generally decouple from the low energy phenomena [2]. If the EWSB sector is strongly interacting instead, in lack of phenomenologically viable models for the strong dynamics [3], the effective field theory approach [4] provides the most general and economic description. In this case, the non-decoupling property of the electroweak sector enforces the new physics scale (Λ) to lie below or at $4\pi v \simeq 3.1$ TeV, where v is the vacuum expectation value characterizing the EWSB.

Below the possible heavy resonances [5] at the scale Λ, the new physics effects in the non-decoupling scenario can be systematically parametrized as the next-to-leading order (NLO) operators of the electroweak chiral Lagrangian (EWCL) [6]. There are in total fifteen NLO bosonic operators, which can modify the electroweak gauge boson interactions and induce the so-called "anomalous couplings" [7]. The contributions of all these NLO operators to various high energy processes have been recently classified by means of a global power counting analysis [8]. Five operators contain quartic gauge couplings (QGCs) which can involve the pure Goldstone boson interactions (according to the equivalence theorem [9]) and are thus of special importance for probing the EWSB. They are summarized as follows [6]:

$$\left\{ \begin{array}{lcl} \mathcal{L}_4 &=& \ell_4 \left(\frac{v}{\Lambda}\right)^2 [\mathrm{Tr}(\mathcal{V}_\mu \mathcal{V}_\nu)]^2 \ , \\ \mathcal{L}_5 &=& \ell_5 \left(\frac{v}{\Lambda}\right)^2 [\mathrm{Tr}(\mathcal{V}_\mu \mathcal{V}^\mu)]^2 \ ; \end{array} \right\} \qquad (SU(2)_c\text{−conserving})$$

$$\left\{ \begin{array}{lcl} \mathcal{L}_6 &=& \ell_6 \left(\frac{v}{\Lambda}\right)^2 [\mathrm{Tr}(\mathcal{V}_\mu \mathcal{V}_\nu)]\mathrm{Tr}(\mathcal{T}\mathcal{V}^\mu)\mathrm{Tr}(\mathcal{T}\mathcal{V}^\nu) \ , \\ \mathcal{L}_7 &=& \ell_7 \left(\frac{v}{\Lambda}\right)^2 [\mathrm{Tr}(\mathcal{V}_\mu \mathcal{V}^\mu)]\mathrm{Tr}(\mathcal{T}\mathcal{V}_\nu)\mathrm{Tr}(\mathcal{T}\mathcal{V}^\nu) \ , \\ \mathcal{L}_{10} &=& \ell_{10} \left(\frac{v}{\Lambda}\right)^2 \frac{1}{2}[\mathrm{Tr}(\mathcal{T}\mathcal{V}^\mu)\mathrm{Tr}(\mathcal{T}\mathcal{V}^\nu)]^2 \ ; \end{array} \right\} \qquad (SU(2)_c\text{−violating}) \qquad (1)$$

where $\mathcal{V}_\mu \equiv (D_\mu U)U^\dagger$, $D_\mu U = \partial_\mu U + \mathbf{W}_\mu U - U\mathbf{B}_\mu$, $\mathbf{W}_\mu \equiv igW^a_\mu \tau^a/2$, $\mathbf{B}_\mu \equiv ig'B_\mu \tau^3/2$, $U = \exp[i\tau^a\pi^a/v]$, and $\mathcal{T} \equiv U\tau_3 U^\dagger$; π^a is the would-be Goldstone boson field and W^a_μ, B_μ the gauge fields of the $SU(2) \otimes U(1)$ group. Note that the operators $\mathcal{L}_{6,7,10}$ violate the custodial $SU(2)_c$ symmetry even in the limit $g' \to 0$. No current experiment ever reaches the sufficient energy threshold to directly probe these five operators which involve only

QGCs. Some roughly estimated bounds were derived through the 1-loop contributions[1] to the Z-pole measurements by keeping only the logarithmic terms. For $\Lambda = 2$ TeV and keeping only one parameter to be non-zero at a time, the 90% C.L. bounds are [10]:

$$\begin{array}{ccc} -4 \leq \ell_4 \leq 20 \ , & -10 \leq \ell_5 \leq 50 \ ; \\ -0.7 \leq \ell_6 \leq 4 \ , & -5 \leq \ell_7 \leq 26 \ , & -0.7 \leq \ell_{10} \leq 3 \ . \end{array} \tag{2}$$

Note that in (1) the dependence on v and Λ is factorized out so that the dimensionless coefficient ℓ_n (for the operator $\mathcal{L}_n$) is naturally of $O(1)$ [4]. The bounds in (2) on the $SU(2)_c$ symmetric parameters $\ell_{4,5}$ are about an order of magnitude above their natural size; while the allowed range for the $SU(2)_c$-breaking parameters ℓ_{6-10} is about a factor of $O(10-100)$ larger than that for $\ell_0 = \frac{\Lambda^2}{2v^2}\Delta\rho \left(= \frac{\Lambda^2}{2v^2}\alpha T\right)$ derived from the ρ (or T [11]) parameter: $0.052 \leq \ell_0 \leq 0.12$ [8], for the same Λ and confidence level. To directly test the EWSB dynamics, it is therefore important to probe these QGCs at future high energy scattering processes where their contributions can be greatly enhanced due to the sensitive power-dependence on the scattering energy [8].

In this Letter, we study the sensitivity of the high energy e^+e^- linear colliders (LCs) with polarized beams to testing these QGCs via the WWZ/ZZZ-production processes. The interplay of these processes with the W-pair production from WW-fusion is analyzed.

2. Relations to Strongly-Interacting Models

Although the fundamental theory behind the effective EWCL is yet unknown, it is important to examine how a typical strongly-interacting electroweak model would contribute to these EWSB parameters. We shall concentrate on the quartic gauge couplings (ℓ_n's) in (1) and consider a few representative models which may contain an isosinglet scalar S, an isotriplet vector V_μ^a, an isotriplet axial vector A_μ^a, and new heavy chiral fermions.

A Non-SM Singlet Scalar

Up to dimension-4 and including both the $SU(2)_c$ conserving and breaking effects, we can write down the most general Lagrangian for an isosinglet scalar:

$$\begin{aligned} \mathcal{L}_{\rm eff}^S \ = \ & \frac{1}{2}\left[\partial^\mu S \partial_\mu S - M_S^2 S^2\right] - V(S) \\ & - \left[\frac{\kappa_s}{2} v S + \frac{\kappa_s'}{4} S^2\right] {\rm Tr}\left[\mathcal{V}_\mu \mathcal{V}^\mu\right] - \left[\frac{\tilde{\kappa}_s}{2} v S + \frac{\tilde{\kappa}_s'}{4} S^2\right] \left[{\rm Tr}\mathcal{T}\mathcal{V}_\mu\right]^2 \end{aligned} \tag{3}$$

where $V(S)$ contains only the self-interactions of the scalar S. The SM Higgs scalar corresponds to a special parameter-choice: $\kappa_s = \kappa_s' = 1$, $\tilde{\kappa}_s = \tilde{\kappa}_s' = 0$ and $V(S) = V(S)_{\rm SM}$.

[1] This is already at the level of $\frac{1}{16\pi^2}\frac{v^2}{\Lambda^2} \lesssim \frac{v^4}{\Lambda^4}$, i.e., of the two-loop order.

When the scalar mass (M_S) is heavy, S can be integrated out from the low energy spectrum with its effects formulated in the heavy mass expansion:

$$\widehat{\mathcal{L}}^S_{\rm eff} \;=\; \frac{v^2}{8M_S^2}\left[\kappa_s {\rm Tr}\left(\mathcal{V}_\mu \mathcal{V}^\mu\right) + \tilde{\kappa}_s {\rm Tr}\left(\mathcal{T}\mathcal{V}_\mu\right)^2\right]^2 + O\left(\frac{1}{M_S^4}\right) \tag{4}$$

After identifying $\Lambda = M_S$ and comparing with (1), we obtain

$$\ell_4^s = 0\ , \quad \ell_5^s = \frac{\kappa_s^2}{8} \geq 0\ ; \qquad \ell_6^s = 0\ , \quad \ell_7^s = \frac{\kappa_s\tilde{\kappa}_s}{4}\ , \quad \ell_{10}^s = \frac{\tilde{\kappa}_s^2}{8} \geq 0\ . \tag{5}$$

In the SM, the only non-zero coupling at the tree level is $(\ell_5^s)_{\rm SM} = 0.125$; while for a different coupling choice: $\kappa_s = -\tilde{\kappa}_s = 2$, we would have $\ell_5^s = 0.5$, $\ell_7^s = -2\ell_{10}^s = -1$.

Vector and Axial-Vector Bosons

The LEP-I Z-pole measurement on the S-parameter disfavors the naive QCD-like technicolor dynamics [11], where the vector particle $\rho_{\rm TC}$ (technirho) is the lowest new resonance in the TeV regime. In modeling the non-QCD-like dynamics, it was suggested [12] that the coexistence of nearly degenerate vector and axial-vector bosons may provide sufficient cancellation for avoiding large corrections to the S-parameter. We thus consider both the vector fields V_μ^a and the axial-vector fields A_μ^a, as isospin triplets of the custodial $SU(2)_c$. Under the global $SU(2)_c$, V and A transform as

$$\widehat{V}_\mu \Rightarrow \widehat{V}'_\mu = \Sigma_v \widehat{V}_\mu \Sigma_v^\dagger\ , \qquad \widehat{A}_\mu \Rightarrow \widehat{A}'_\mu = \Sigma_v \widehat{A}_\mu \Sigma_v^\dagger\ , \tag{6}$$

where $\widehat{V}_\mu \equiv V_\mu^a \tau^a/2$, $\widehat{A}_\mu \equiv A_\mu^a \tau^a/2$, and $\Sigma_v \in SU(2)_c$. If V and A are further regarded as gauge fields of a new local hidden symmetry group $\mathcal{H} = SU(2)'_L \otimes SU(2)'_R$ (with a discrete left-right parity) [12], we can write down the following general Lagrangian (up to two derivatives), in the *unitary gauge*[2] of the group $\mathcal{H}$ and with both $SU(2)_c$-conserving and -breaking effects included,

$$\begin{aligned}\mathcal{L}^{VA}_{\rm eff} = \mathcal{L}^{VA}_{\rm kinetic} - \frac{v^2}{4}\Big[&\kappa_0 {\rm Tr}\mathcal{V}_\mu^2 + \kappa_1 {\rm Tr}\left(J_\mu^V - 2V_\mu\right)^2 + \kappa_2 {\rm Tr}\left(J_\mu^A + 2A_\mu\right)^2 + \kappa_3 {\rm Tr}A_\mu^2\Big] \\ &+\tilde{\kappa}_1\left[{\rm Tr}\tau^3(J_\mu^V - 2V_\mu)\right]^2 + \tilde{\kappa}_2\left[{\rm Tr}\tau^3(J_\mu^A + 2A_\mu)\right]^2 + \tilde{\kappa}_3\left[{\rm Tr}\tau^3 A\right]^2\Big]\end{aligned} \tag{7}$$

with

[2]By "unitary gauge" we mean a gauge containing no new Goldstone bosons other than the three for generating the longitudinal components of the W, Z bosons. In fact, it is not necessary to introduce such a new local symmetry $\mathcal{H}$ for V, A [13] since $\mathcal{H}$ has to be broken anyway and V, A can be treated as matter fields [14]. The hidden local symmetry requires the coefficients of the terms $-J_\mu^V V^\mu$ and $V_\mu V^\mu$ to be the same, due to the additional assumption about that new local group $\mathcal{H}$.

$$\left\{\begin{array}{ll} J_\mu^V = J_\mu^L + J_\mu^R & \left\{\begin{array}{l} J_\mu^L = \xi^\dagger D_\mu^L \xi = \xi^\dagger \left(\partial_\mu + \mathbf{W}_\mu\right) \xi \\ J_\mu^R = \xi D_\mu^R \xi^\dagger = \xi \left(\partial_\mu + \mathbf{B}_\mu\right) \xi^\dagger \end{array}\right. \\ J_\mu^A = J_\mu^L - J_\mu^R & \end{array}\right. \tag{8}$$

and $V_\mu \equiv i\tilde{g}\widehat{V}_\mu = i\tilde{g}V_\mu^a \tau^a/2$, $A_\mu \equiv i\tilde{g}\widehat{A}_\mu = i\tilde{g}A_\mu^a \tau^a/2$, and $\xi \equiv U^{\frac{1}{2}}$, where $\tilde{g}$ is the gauge coupling of the group $\mathcal{H}$. Among the above new parameters (κ_n's), κ_0 is determined by normalizing the Goldstone boson kinetic term: $\kappa_0 = -4\kappa_2\kappa_3/(4\kappa_2+\kappa_3)$. After eliminating the V and A fields in the heavy mass expansion, we obtain

$$\begin{aligned} \widehat{\mathcal{L}}_{\rm eff}^{VA} &= \frac{(\eta^2-1)^2+16\tilde{\eta}^2}{8\tilde{g}^2}\left[\left(\mathrm{Tr}\mathcal{V}_\mu\mathcal{V}_\nu\right)^2 - \left(\mathrm{Tr}\mathcal{V}_\mu\mathcal{V}^\mu\right)^2\right] + \\ &\quad \frac{\tilde{\eta}\left(4(3-\eta^2)\tilde{\eta}+(1-\eta^2)\eta\right)}{8\tilde{g}^2}\left[\mathrm{Tr}\mathcal{V}_\mu^2\left(\mathrm{Tr}\mathcal{T}\mathcal{V}_\nu\right)^2 - \mathrm{Tr}\left(\mathcal{V}_\mu\mathcal{V}_\nu\right)\mathrm{Tr}\left(\mathcal{T}\mathcal{V}^\mu\right)\mathrm{Tr}\left(\mathcal{T}\mathcal{V}^\nu\right)\right] + O\left(\frac{1}{M_{V,A}^4}\right) \end{aligned} \tag{9}$$

which contributes to ℓ_n as follows:

$$\left\{\begin{array}{ll} \ell_4 = \ell_4^v + \ell_4^a & \left\{\begin{array}{l} \ell_4^v = -\ell_5^v = 1/[2\sqrt{2}\tilde{g}v\Lambda^{-1}]^2 > 0 \\ \ell_4^a = -\ell_5^a = \left[\eta^2(\eta^2-2)+16\tilde{\eta}^2\right]/[2\sqrt{2}\tilde{g}v\Lambda^{-1}]^2 \\ \ell_6^v = \ell_7^v = 0 \\ \ell_6^a = -\ell_7^a = -\tilde{\eta}\left[4(3-\eta^2)\tilde{\eta}+(1-\eta^2)\eta\right]/[2\sqrt{2}\tilde{g}v\Lambda^{-1}]^2 \\ \ell_{10}^v = \ell_{10}^a = 0 \end{array}\right. \\ \ell_5 = \ell_5^v + \ell_5^a & \\ \ell_6 = \ell_6^v + \ell_6^a & \\ \ell_7 = \ell_7^v + \ell_7^a & \\ \ell_{10} = \ell_{10}^v + \ell_{10}^a & \end{array}\right. \tag{10}$$

where

$$\eta = \frac{4\kappa_2}{4\kappa_2+\kappa_3}\,, \qquad \tilde{\eta} = \frac{2\kappa_2+4\tilde{\kappa}_2}{(4\kappa_2+\kappa_3)+2\left(4\tilde{\kappa}_2+\tilde{\kappa}_3\right)} - \frac{2\kappa_2}{4\kappa_2+\kappa_3}\,, \tag{11}$$

and $\Lambda = \min(M_V, M_A)$. At the leading order, $(M_V, M_A) \simeq \left(\tilde{g}v\sqrt{\kappa_1},\ \tilde{g}v\sqrt{\kappa_2+\kappa_3/4}\right)$, after ignoring the SM gauge couplings g and g'. In (10), the factor $1/[\tilde{g}v\Lambda^{-1}]^2 \simeq \kappa_1(\Lambda/M_V)^2 = O(\kappa_1)$ and all $SU(2)_c$-breaking terms depend on $\tilde{\eta}$. We see that the $SU(2)_c$-symmetric contribution from the axial-vector boson interactions to $\ell_4^a = -\ell_5^a$ becomes negative for $|\eta| < \sqrt{2}$, while the summed contribution $\ell_4 = -\ell_5 = \left[(\eta^2-1)^2+16\tilde{\eta}^2\right]/[2\sqrt{2}\tilde{g}v\Lambda^{-1}]^2 \geq 0$. The deviation of η and/or $\tilde{\eta}$ from $\eta(\tilde{\eta}) = 0$ represents the *non-QCD-like* EWSB dynamics. For instance, in the case of $\tilde{g} = 3$ and $\{\eta, \tilde{\eta}\} = \{1.5, -0.25\}$, we have $\ell_4 = -\ell_5 = 2.35$, $\ell_6 = -\ell_7 = -0.60$, $\ell_{10} = 0$ for $\Lambda = 2$ TeV.

Heavy Fermion Doublet

Consider a simple model with two heavy chiral fermions in the fundamental representation of a new strong $SU(N)$ gauge group. They form a left-handed weak doublet $(U_L, D_L)^T$ and right-handed singlets (U_R, D_R). The small mass-splitting of fermions U and D breaks the $SU(2)_c$ and is characterized by the parameter $\omega = 1 - (M_D/M_U)^2$. The anomaly-cancellation is ensured by assigning the U, D electric charges as $(+\frac{1}{2}, -\frac{1}{2})$. By taking

(U, D) as the source of the EWSB, the W, Z masses can be generated by heavy fermion loops. The new contributions to the quartic gauge couplings of W/Z come from the *non-resonant* (U, D) box-diagrams[3]. The leading results in the $1/M_{U,D}$ and ω expansions are derived as follows:

$$\ell_4^f = -2\ell_5^f = \left(\frac{\Lambda}{4\pi v}\right)^2 \frac{N}{12} \; ; \quad \ell_6^f = -\ell_7^f = -\left(\frac{\Lambda}{4\pi v}\right)^2 \frac{7N}{240}\omega^2 \; , \quad \ell_{10} = 0 \; ; \tag{12}$$

where $\Lambda = \min(M_U, M_D)$. For a model with $N = 4$ and $(M_U, M_D) = (3.1, 3.0)$ TeV, *i.e.*, $\Lambda = 3$ TeV and $\omega = 0.063$, we have $\ell_4^f = -2\ell_5^f \simeq 0.33$, and $\ell_6^f = -\ell_7^f \simeq 0$.

In summary, the typical values of the QGCs (ℓ_n's) are expected to be around $O(1)$, and different models of the strongly-interacting EWSB sector result in different patterns of these parameters. In the following sections we study the direct test of the QGCs at the high energy linear colliders and show how the bounds can be improved in order to sensitively discriminate different models.

3. Testing Quartic Gauge Boson Couplings via WWZ/ZZZ-Production

While the CERN Large Hadron Collider (LHC) may provide the direct test on these new quartic gauge couplings (QGCs) through WW fusion processes, the large SM backgrounds make the experimental measurements difficult [5]. The corresponding studies for the fusion processes at the TeV $e^{\pm}e^{-}$ linear colliders show that the complementary information can be obtained [16, 17]. On the other hand, the triple gauge boson production processes

$$e^+e^- \longrightarrow W^+W^-Z, \quad ZZZ \tag{13}$$

have large cross sections just above the threshold [18] and may prove to be useful for probing the QGCs [19], which contribute to the signal diagrams involving s-channel Z-boson. In this section, we make a systematic analysis on the above processes and demonstrate the crucial role of the polarized $e^{\mp}$ beams.

Because of the relatively clean experimental environment at the LC, we identify the final state W/Z's via their hadronic dijet modes. Due to the limited calorimeter energy resolution, the misidentification probability of W versus Z should be considered [16]. To increase the statistics, we also add the clean channel $Z \to \mu^-\mu^+$. To avoid other potential backgrounds of the type $e^-e^+ \to eeZZ, eeWW$, the electron-pair mode of Z-decay is not

[3]These box-diagrams were computed for the SM fermions in Ref. [15].

included. We find that the detection efficiencies for WWZ and ZZZ final states are about 18.4% and 16.8%, respectively. It turns out that the t-channel ν_e exchange diagrams in $e^-e^+ \to WWZ$ production pose a large SM background to the QGC signal, and they can hardly be suppressed by simple kinematic cuts alone (cf. Fig. 1). However, we note that such a type of background involves the left-handed W-e-ν coupling and thus can be very effectively suppressed by using the right(left)-handed polarized $e^-(e^+)$ beam. The highest sensitivity is reached by maximally polarizing *both* e^- and e^+ beams. This is shown in Fig. 1 for distributions of the invariant mass M_{WW}, transverse momentum $p_T(Z)$ and $\cos\theta(e^-Z)$ at the 500 GeV LC, without/with beam polarizations. To enhance the signal-to-background ratio, we also impose some kinematical cuts as indicated by the vertical lines in each panel of Fig. 1.

The crucial roles of the beam polarization and the higher collider energy for the WWZ-production are demonstrated in Fig. 2a, where $\pm 1\sigma$ exclusion contours for ℓ_4-ℓ_5 are displayed at $\sqrt{s} = 0.5,\ 0.8,\ 1.0$ and 1.6 TeV, respectively. The beam polarization has much less impact on the ZZZ mode, due to the almost axial-vector type e-Z-e coupling. Including the same polarizations as in the case of the WWZ mode, we find about $10 - 20\%$ improvements on the bounds from the ZZZ-production. Assuming the two beam polarizations (90% e^- and 65% e^+), we summarize the final $\pm 1\sigma$ bounds for both ZZZ and WWZ channels and their combined 90% C.L. contours for 0.5 TeV with $\int \mathcal{L} = 50$ fb^{-1} in Fig. 2b (representing the *first direct probe* at the LC) and for 1.6 TeV with $\int \mathcal{L} = 200$ fb^{-1} in Fig. 2c (representing the *best* sensitivity gained from the final stage of the LC with energy around 1.5/1.6 TeV). We see that, at the 90% C.L. level, the bounds on ℓ_4-ℓ_5 at 0.5 TeV are within $O(10 - 20)$, while at 1.6 TeV they sensitively reach $O(1)$. The ellipses for the WWZ final state in ℓ_4-ℓ_5 plane are identical to those in ℓ_6-ℓ_7 plane, while the bands for the ZZZ final state in ℓ_6-ℓ_7 plane become tighter due to a factor of 2 enhancement from the $4Z$-interaction vertex. ℓ_{10} only contributes to ZZZ final state and can be probed at the similar level. The new physics cutoff is chosen as $\Lambda = 2$ TeV in our plots and the numerical results for other values of Λ can be obtained by simple scaling. In the above, the total rates are used to derive the numerical bounds. We have further studied the possible improvements by including different characteristic distributions (cf. Fig. 1), but no significant increase of the sensitivity is found for the above processes.

Finally, a parallel analysis to Fig. 2b-c has been carried out for the situation without

e^+ beam polarization (with e^- polarization as before). For a two-parameter ($\ell_{4,5}$) study, the 90% C.L. results are compared as folllows:

$$\begin{array}{lll} \text{at 0.5 TeV :} & -12\ (-18) \le \ell_4 \le 21\ (27), & -17\ (-22) \le \ell_5 \le 9.5\ (15); \\ \text{at 1.6 TeV :} & -0.50\ (-0.67) \le \ell_4 \le 1.5\ (1.7), & -1.3\ (-1.5) \le \ell_5 \le 0.36\ (0.58); \end{array} \tag{14}$$

where the numbers in the parentheses denote the bounds from polarizing the e^--beam alone. The comparison in (14) shows that without e^+-beam polarization, the sensitivity will decrease by about $15\% - 60\%$. Therefore, making use of the possible e^+-beam polarization with a degree around 65% will certainly be beneficial.

4. Interplay of WWZ/ZZZ-Production and WW-Fusion

The scattering amplitudes of the longitudinally polarized $WW \to WW$ fusion have the highest power dependence on the scattering energy E, while the s-channel WWZ/ZZZ production at higher energies suffers a reduction factor of $(v/E)^2$ relative to that of the fusion processes [8]. When the collider energy is reduced by half (from 1.6 TeV down to 800 GeV), the sensitivity of the WW-fusion decreases by about a factor of 20 or more [17]. We therefore expect that $e^-e^+ \to WWZ, ZZZ$ are more important at the earlier phase of the linear collider and will be competitive with and complementary to the WW-fusion for later stages with energies $\sim 0.8 - 1$ TeV. At even higher energies $\sim$1.5/1.6 TeV, the fusion processes will take over due to their higher energy dependence. The following analysis reveals that even at 1.6 TeV, $e^-e^+ \to WWZ$ plays a crucial role for probing the $SU(2)_c$-breaking parameters (ℓ_6, ℓ_7).

For WW-fusion processes, there are five useful channels to consider:

$$\begin{array}{lll} \text{Full process :} & \text{Subprocess :} & \text{Parameter dependence :} \\ e^-e^+ \to \nu\bar{\nu}W^-W^+\ , & (W^-W^+ \to W^-W^+), & (\ell_{4,5})\ , \\ e^-e^- \to \nu\bar{\nu}W^-W^-\ , & (W^-W^- \to W^-W^-), & (\ell_{4,5})\ ; \\ e^-e^+ \to \nu\bar{\nu}ZZ\ , & (W^-W^+ \to ZZ), & (\ell_{4,5};\ \ell_{6,7})\ , \\ e^-e^+ \to e^\pm\nu W^\mp Z\ , & (W^\mp Z \to W^\mp Z), & (\ell_{4,5};\ \ell_{6,7})\ , \\ e^-e^+ \to e^-e^+ZZ\ , & (ZZ \to ZZ), & ([\ell_4 + \ell_5] + 2[\ell_6 + \ell_7 + \ell_{10}])\ . \end{array} \tag{15}$$

The first two processes in (15) only involve $\ell_{4,5}$ and thus can provide a clean test on them. Including the third and fourth reactions, one may further probe $\ell_{6,7}$. Finally the fifth channel provides information on ℓ_{10}. However, the realistic situation is more involved. First of all, the WZ-channel has large γ-induced backgrounds $e\gamma \to \nu WZ$ and $\gamma\gamma \to WW$.

Secondly, the small electron neutral-current coupling heavily suppresses the total rate of the $ZZ \to ZZ$ process. Consequently, the sensitivity-bound on ℓ_6-ℓ_7 from the $e\nu WZ$ channel is significantly weaker than that from the $\nu\bar{\nu}ZZ$ channel [17], as illustrated in Fig. 3. On the other hand, the triple gauge boson process $e^-e^+ \to WWZ$ provides complementary information. Fig. 3a demonstrates the interplay of WW-fusion and WWZ-production for discriminating the $SU(2)_c$-breaking parameters ℓ_6-ℓ_7 at a 1.6 TeV LC with 200 fb^{-1} luminosity. The sensitivity of WWZ channel is shown to be comparable with $\nu\bar{\nu}ZZ$ fusion channel in probing $\ell_{6,7}$. Here the bound from νeWZ channel is relatively too weak to be useful. Including the WWZ channel, the bound on $\ell_{6,7}$ is improved by about a factor of 2 and thus reaches the same level as that of $\ell_{4,5}$ derived from the $\nu\bar{\nu}W^-W^+$ and $\nu\nu W^-W^-$ channels [17]. To constrain ℓ_{10}, both ZZZ and $eeZZ$ channels are available. Assuming that $\ell_{4,5;6,7}$ are constrained by the processes mentioned above, we set their values to be zero (the reference point) for simplicity and define the statistic significance $S = |\mathcal{N} - \mathcal{N}_0|/\sqrt{\mathcal{N}_0}$ which is a function of ℓ_{10}. (Here $\mathcal{N}$ is the total event-number while $\mathcal{N}_0$ is the number at $\ell_{10} = 0$.) As shown in Fig. 3b, at 1.6 TeV, the sensitivity of $e^-e^+ \to eeZZ$ for probing ℓ_{10} is better than that of $e^-e^+ \to ZZZ$.

5. Conclusions

After analyzing the different patterns of the quartic gauge boson couplings in connection with the representative strongly-interacting models, we study the sensitivities in probing both the $SU(2)_c$-symmetric and -breaking QGCs via WWZ/ZZZ-production at the LCs. We summarize in Table 1 the combined 90% C.L. sensitivity bounds on the QGCs from WWZ and ZZZ channels for typical energies and luminosities of the LCs, which are to be compared with the estimated *indirect* LEP-bounds in (2). We further analyze the interplay of the WWZ/ZZZ-production with the WW-fusion mechanism for achieving an improved determination of all the five QGCs. The important roles of both the polarized e^- and e^+ beams for the WWZ-production are revealed and analyzed.

The first direct probe on these QGCs will come from the early phase of the LC at 500 GeV, where the WW-fusion processes are not useful. The two mechanisms become more competitive and complementary at energies $\sqrt{s} \sim 0.8 - 1$ TeV. At a later stage of the LC, $\sqrt{s} = 1.6$ TeV, the 90% C.L. one-parameter bounds from the fusion processes become

very sensitive, for $\Lambda = 2$ TeV:

$$\begin{array}{c} -0.13 \le \ell_4 \le 0.10\ , \quad -0.08 \le \ell_5 \le 0.06\ ; \\ -0.22 \le \ell_6 \le 0.22\ , \quad -0.12 \le \ell_7 \le 0.10\ , \quad -0.21 \le \ell_{10} \le 0.21\ ; \end{array} \tag{16}$$

obtained for $\int \mathcal{L} = 200$ fb^{-1} with a 90% (65%) polarized $e^-(e^+)$ beam. The bounds on $\ell_{4,5}$ are about a factor of $3 \sim 6$ stronger than that from WWZ/ZZZ-modes (cf. Table 1); while the bounds on $\ell_{6,7,10}$ are comparable. For a complete multi-parameter analysis, the WWZ-channel is crucial for determining ℓ_6-ℓ_7 even at a 1.6 TeV LC.

Table 1: Combined 90% C.L. bounds on ℓ_{4-10} from WWZ/ZZZ-production. For simplicity, we set one parameter to be nonzero at a time. The bound on ℓ_{10} comes from ZZZ-channel alone.

$\sqrt{s}$ (TeV)	0.5	0.8	1.0	1.6
$\int \mathcal{L}$ (fb^{-1})	50	100	100	200
	$-9.5 \le \ell_4 \le 11.7$	$-2.7 \le \ell_4 \le 3.2$	$-1.7 \le \ell_4 \le 2.0$	$-0.50 \le \ell_4 \le 0.58$
WWZ/ZZZ	$-9.8 \le \ell_5 \le 8.9$	$-3.1 \le \ell_5 \le 2.3$	$-1.9 \le \ell_5 \le 1.4$	$-0.54 \le \ell_5 \le 0.36$
Bounds	$-5.0 \le \ell_6 \le 5.8$	$-1.5 \le \ell_6 \le 1.6$	$-0.95 \le \ell_6 \le 1.0$	$-0.28 \le \ell_6 \le 0.28$
(at 90%C.L.)	$-5.0 \le \ell_7 \le 5.7$	$-1.5 \le \ell_7 \le 1.5$	$-0.95 \le \ell_7 \le 0.92$	$-0.28 \le \ell_7 \le 0.26$
	$-4.3 \le \ell_{10} \le 5.2$	$-1.4 \le \ell_{10} \le 1.4$	$-0.83 \le \ell_{10} \le 0.88$	$-0.26 \le \ell_{10} \le 0.26$
Range of $\lvert\ell_n\rvert$	$\le O(4 \sim 10)$	$\le O(1 \sim 3)$	$\le O(0.8 \sim 2)$	$\le O(0.3 \sim 0.6)$

Acknowledgments We thank E. Boos, R. Casalbuoni, D. Dominici, G. Jikia, Y.P. Kuang, H.Y. Zhou, I. Kuss, A. Likhoded, C.R. Schmidt, G. Valencia, and P.M. Zerwas for valuable discussions. TH is supported by U.S. DOE under contract DE-FG03-91ER40674 and the Davis Institute for High Energy Physics; HJH by the AvH of Germany; CPY and HJH by the U.S. NSF under grant PHY-9507683.

Note added: After the submission of this paper, we received a paper from O.J.P. Eboli *et al.* [20] who also studied the WWZ/ZZZ production for probing the quartic gauge boson couplings. With different cuts and beam polarization choice, they obtained weaker bounds than ours. They reached a similar conclusion on the role of the e^--polarization for the WWZ-channel.

References

1. D. Bardin *et al*, *Electroweak Working Group Report,* hep-ph/9709229.
2. T. Appelquist and J. Carazzone, Phys. Rev. **D11** (1975) 2856.
3. See, *e.g.*, K. Lane, BUHEP-94-26 and hep-ph/9501249; M. Lindner, hep-ph/9704362; and references therein.
4. For a nice review, H. Georgi, Ann. Rev. Nucl. & Part. Sci. **43** (1994) 209.
5. J. Bagger, V. Barger, K. Cheung, J. Gunion, T. Han, G.A. Ladinsky, R. Rosenfeld, and C.-P. Yuan, Phys. Rev. **D49** (1994) 1246; **D52** (1995) 3878.
6. T. Appelquist and C. Bernard, Phys. Rev. **D22** (1980) 200; A.C. Longhitano, Nucl. Phys. **B188** (1981) 118.
7. K. Hagiwara *et al.*, Nucl. Phys. **B282** (1987) 253. For recent reviews, *e.g.*, H. Aihara *et al.*, DPF Rep., hep-ph/9503425; T. Barklow et al, (Snowmass-96), hep-ph/9611454.
8. H.-J. He, Y.-P. Kuang, C.-P. Yuan, hep-ph/9708402; Phys. Rev. **D55** (1997) 3038; Mod. Phys. Lett. **A11** (1996) 3061; Phys. Lett. **B382** (1996) 149; for an updated review, hep-ph/9704276.
9. H.-J. He, Y.-P. Kuang, and C.-P. Yuan, Phys. Rev. **D51** (1995) 6463; H.-J. He, and W.B. Kilgore, *ibid.* **D55** (1997) 1515; H.-J. He, et al, *ibid.* **D49** (1994) 4842; Phys. Lett. **B329** (1994) 278; Phys. Rev. Lett. **69** (1992) 2619; and references therein.
10. O.J.P. Eboli *et al.*, Phys. Lett. **B339** (1995) 119; **B375** (1996) 233; S. Dawson and G. Valencia, Nucl. Phys. **B439** (1995) 3.
11. M.E. Peskin and T. Takeuchi, Phys. Rev. Lett. **65** (1990) 964.
12. R. Casalbuoni *et al.*, Phys. Rev. **D53** (1996) 5201, and references therein.
13. H. Georgi, Nucl. Phys. **B331** (1990) 311.
14. C.G. Callan, S. Coleman, J. Wess, and B. Zumino, Phys. Rev. **177** (1969) 2247.
15. A. Masiero *et al.*, Phys. Lett. **B355** (1995) 329.
16. V. Barger, K. Cheung, T. Han, and R.J.N. Phillips, Phys. Rev. **D52** (1995) 3815; T. Han, hep-ph/9704215, in the proceedings of *The Higgs Puzzle,* Ringberg, Germany, December 8-13, 1996, pp.197-206, ed. B. Kniehl (World Scientific).
17. H.-J. He, DESY-97-037, in the proceedings of *The Higgs Puzzle,* Ringberg, Germany, December 8-13, 1996, pp.207-217, ed. B. Kniehl (World Scientific); E. Boos, H.-J. He, W. Kilian, A. Pukhov, C.-P. Yuan, and P.M. Zerwas, hep-ph/9708310 and

Phys. Rev. **D57** (1998) No. 3 (in press).

18. V. Barger and T. Han, Phys. Lett. **B212** (1988) 117; V. Barger, T. Han, and R.J.N. Phillips, Phys. Rev. **D39** (1989) 146.
19. G. Belanger and F. Boudjema, Phys. Lett. **B288** (1992) 201; S. Godfrey, in *International Symposium on Vector Boson Self-Interactions,* pp.209-223, Los Angles, Feb 6-8, 1995, hep-ph/9505252; S. Dawson, A. Likhoded, G. Valencia, O. Yuschenko, (Snowmass-1996), hep-ph/9610299.
20. O.J.P. Eboli, M.C. Gonzalez-Garcia, and J.K. Mizukoshi, hep-ph/9711499.

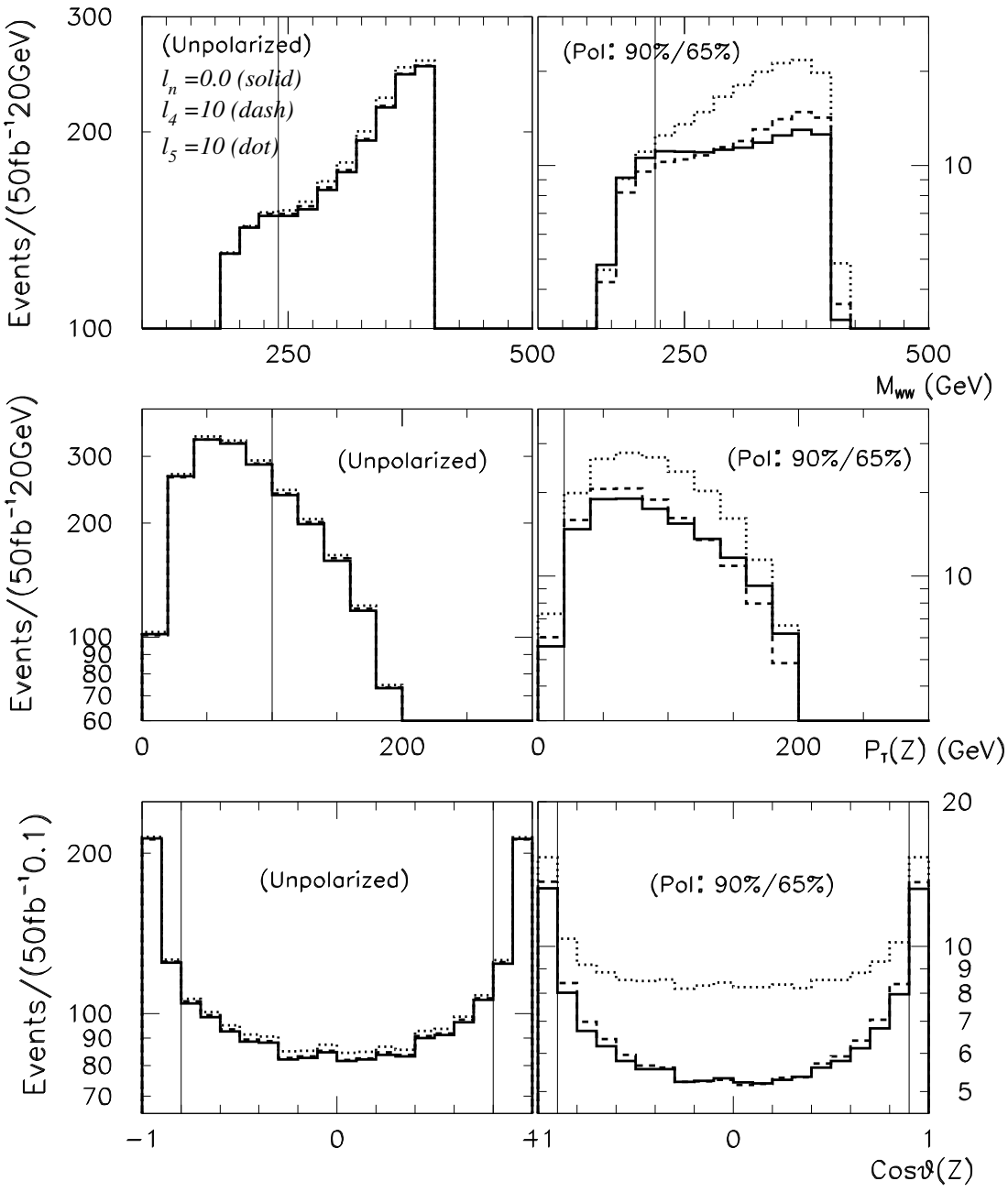

Figure 1: Kinematical distributions and cuts (indicated by the vertical lines in each panel) for $e^-e^+ \to WWZ$ at 0.5 TeV with an integrated luminosity 50 fb^{-1}. Results with $\ell_n = 0$ (solid), $\ell_4 = 10$ (dashes) and $\ell_5 = 10$ (dotted) are shown. The left and right panels compare the results without and with beam polarizations.

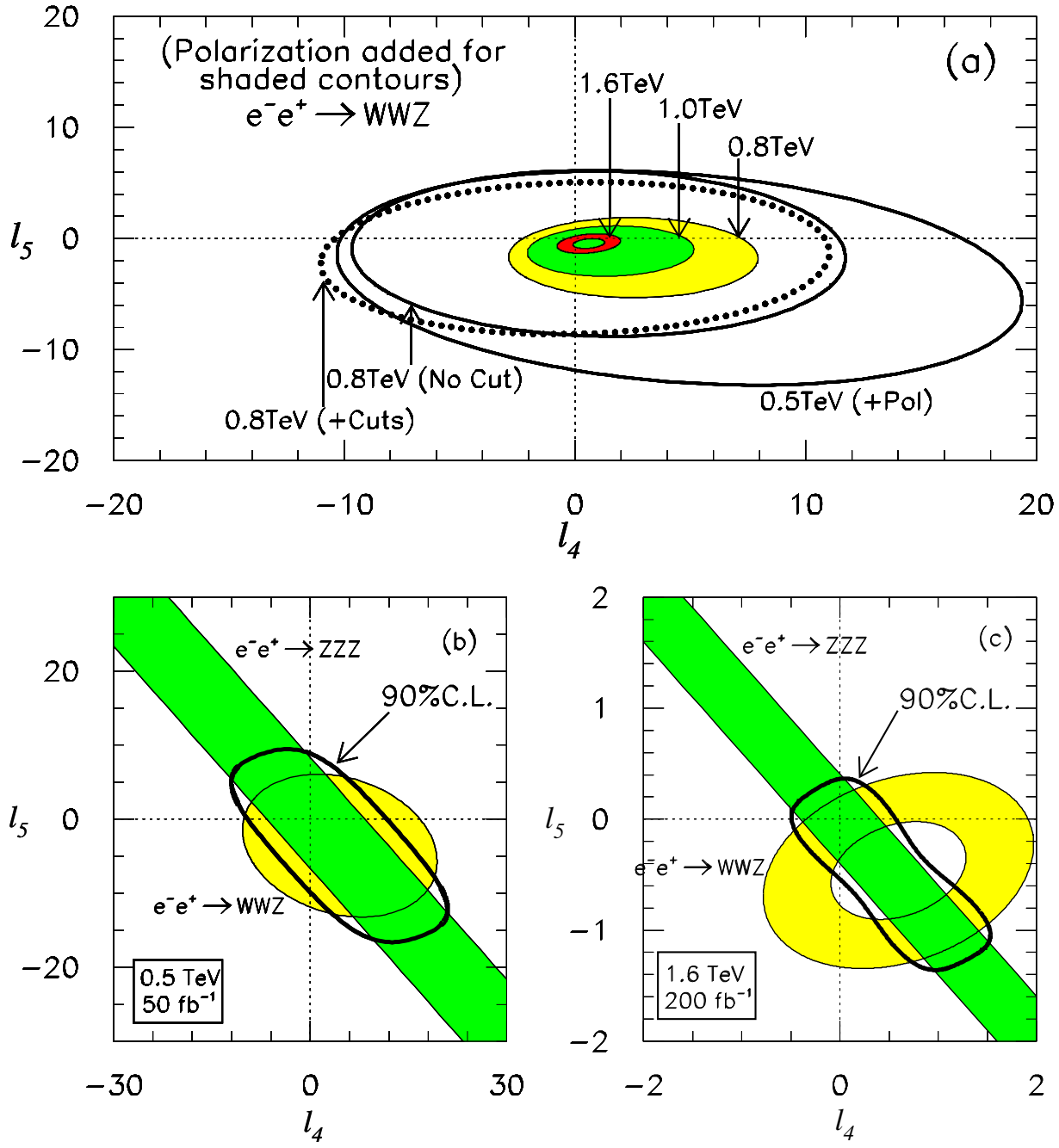

Figure 2: Probing ℓ_4-ℓ_5 via WWZ and ZZZ production processes. The roles of the polarization and the higher collider energy for $e^-e^+ \to WWZ$ are shown by the $\pm 1\sigma$ exclusion contours in (a). The integrated luminosities used here are 50 fb^{-1} (at 500 GeV), 100 fb^{-1} (at 800 GeV) and 200 fb^{-1} (at 1.0 and 1.6 TeV). In (b) and (c), the $\pm 1\sigma$ contours are displayed for ZZZ/WWZ final states at $\sqrt{s}$ =0.5 and 1.6 TeV respectively, with two beam polarizations (90% e^- and 65% e^+); the thick solid lines present the combined bounds at 90% C.L.

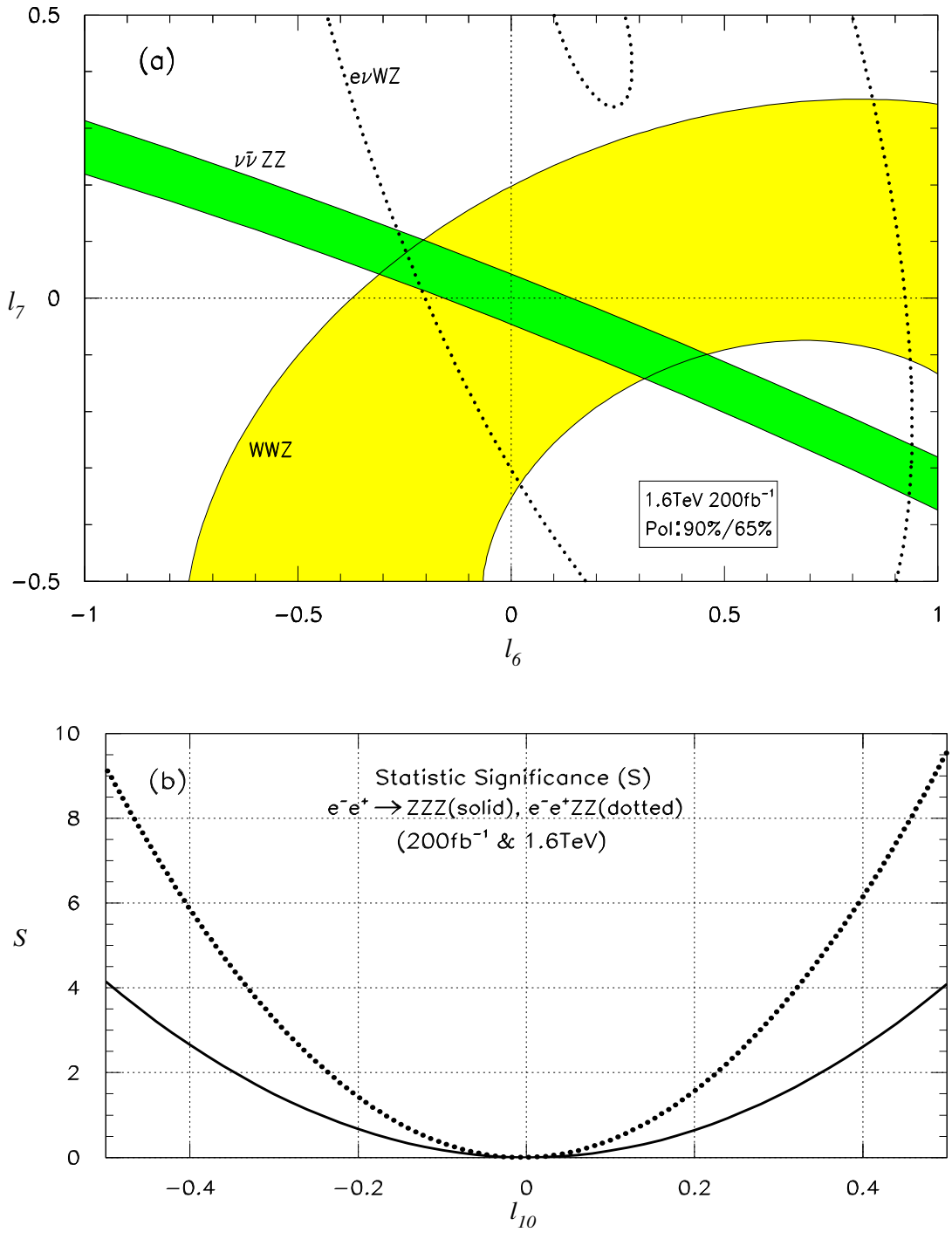

Figure 3: Interplay of the WW-fusion and WWZ/ZZZ-production for discriminating ℓ_6-ℓ_7 and ℓ_{10} at $\sqrt{s}$ =1.6 TeV with $\int \mathcal{L}$ =200 fb^{-1}: (a). $\pm 1\sigma$ exclusion contours for $e^-e^+ \to \nu\bar{\nu}ZZ$, $e^+\nu W^-Z/e^-\bar{\nu}W^+Z$, and $e^-e^+ \to WWZ$ with polarizations (90% e^- and 65% e^+). (b). Statistic significance versus ℓ_{10} for $e^-e^+ \to ZZZ$, e^-e^+ZZ (with unpolarized $e^\mp$ beams).